Supporting Information

Mercury Removal from Wastewater using Cysteamine Functionalized Membrane

Mohammad Saiful Islam[1], Ronald J. Vogler[1], Sayed Mohammad Abdullah Al Hasnine[2], Sebastián Hernández[1], Nga Malekzadeh[3], Thomas P. Hoelen[3], Evan S. Hatakeyama[3] and Dibakar Bhattacharyya[1]*

[1]Department of Chemical and Materials Engineering, University of Kentucky, Lexington, KY

[2]Department of Mechanical Engineering, University of Kentucky, Lexington, KY

[3]Chevron Energy Technology Company, Richmond, CA

*Corresponding Author

S1. Industrial Wastewater Quality

The wastewater was collected from an industrial site in California. Wastewater has the following composition shown in **Table S1**. However, the HgS and Hg^{2+} quantities varied from stream to stream and with time. The wastewater was spiked with an additional 200 ppb of HgS (average hydrodynamic diameter 20~30 nm by DLS) and 110 ppb Hg^{2+} (added as $Hg(NO_3)_2 \cdot xH_2O$ (x = 1−2)) for adsorption experiments using thiol functionalized membranes, which was needed to allow for quantitative measurements of removal efficiencies. The resulting total HgS NP and dissolved Hg^{2+} was approximately 200 ppb and 110 ppb, respectively. The suspension of HgS nanoparticls (NPs) (1 ppm) was received on January 25, 2018 from Dr. Gregory V. Lowry (Carnegie Mellon University, Pittsburgh, PA).

Table S1. Constituents of wastewater as tested

Name of the Compound	Amount (ppm)	Method Used
As HgS	80% HgS NPs ≤ 20~30 nm	DLS
As Hg^{2+}	0.001 to 0.050	Mercury Analyzer and ICP-OES
As Na	~357	ICP-OES
As Mg	25~26	ICP-OES
As Ca	52	ICP-OES
As K	~17	ICP-OES
TOC	0~4	TOC Analyzer
TDS	<2000	TDS Meter
pH	~7	pH Meter

S2. Proposed Treatment Process to Remove Mercury from Wastewater

Based on the quality of the industrial effluent water (**Table S1**) three steps treatment process was proposed demonstrated in **Figure S1**. The first step is primary filtration using PVDF membrane to remove large impurities. In the second step PS35 ultrafiltration membrane was used to remove HgS NPs and, finally thiol functionalized membrane was used to adsorb dissolved Hg^{2+} from wastewater.

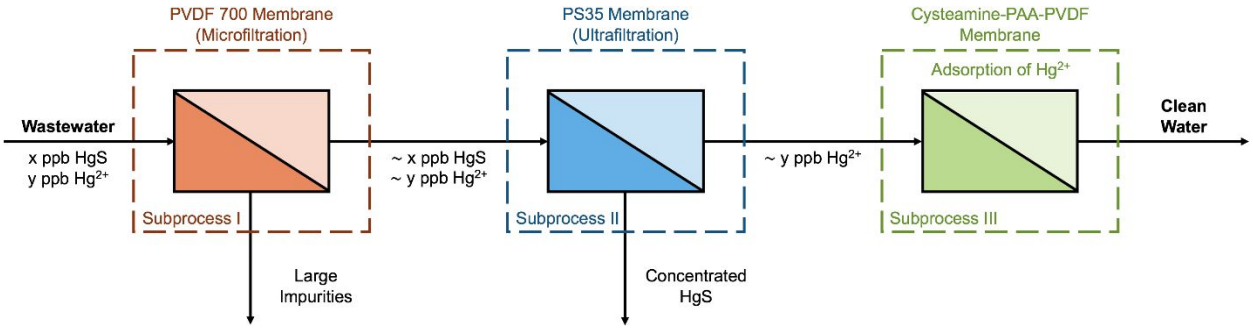

Figure S1: Proposed treatment process for removal of mercury (HgS Nanoparticles, dissolved Hg^{2+}) from wastewater. The values of the concentration of HgS and Hg^{2+} in this graphic is just to represent arbitrary concentration. Depending on the source of wastewater x and y can vary.

S3. Primary Filtration to Remove Particulates from Wastewater using PVDF Membrane

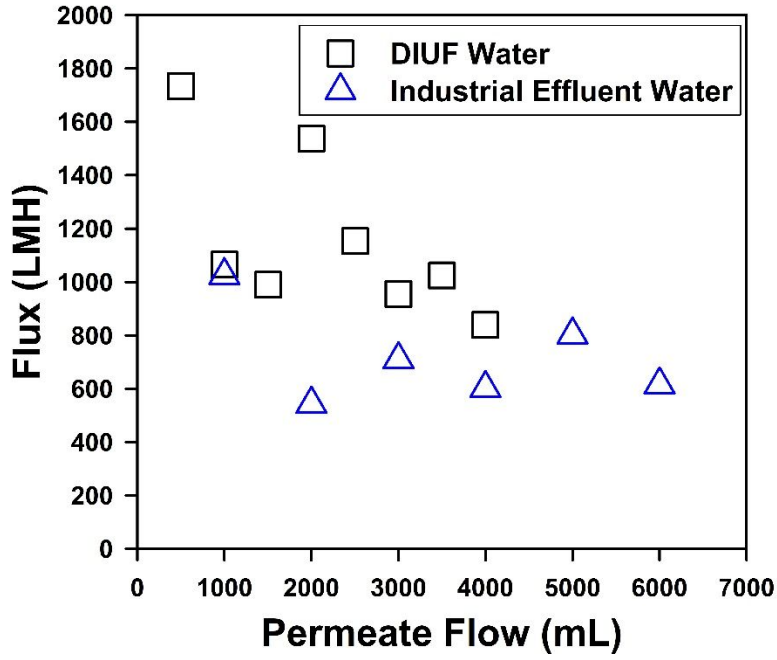

(a)

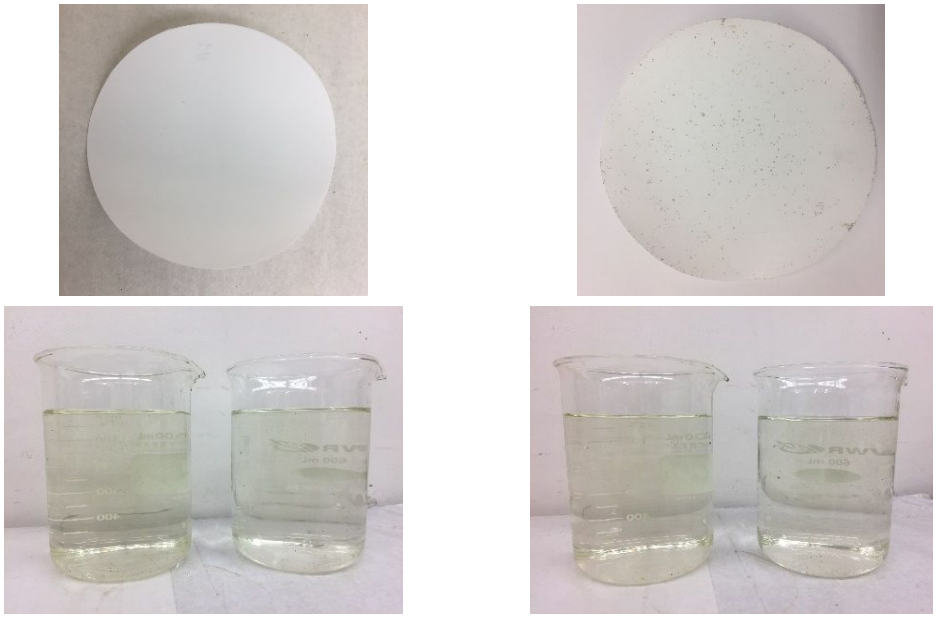

(b)

Figure S2: (a) Flux profile for DIUF and wastewater using PVDF membrane for initial filtration to remove particulates. Effective membrane surface area is 65.03 cm^2. **(b)** Images of membrane used and wastewater condition before and after initial filtration.

Table S2. Detail data of membrane used for HgS nanoparticle separation

Manufacturer	Nanostone
Types of membrane	Ultrafiltration
Membrane reference	PS35
MWCO	20 kDa
pH process limits	2 - 10
Membrane area	13.2 cm^2

S4. ATR-FTIR Spectra Analysis of Functionalized Membranes

Analyzing the absorption peaks of fluorocarbons, carboxyl, amine and thiol groups will ascertain the functionality of each step. The ATR-FTIR spectrum during measurement was set between 400 and 4000 cm^{-1}. The built-in OMNIC software was used with the instrument to set and record the parameters of measurement. The resolution was set to a value of 4 cm^{-1}, the number of scans was 64 respectively during FTIR measurement. The samples were placed on a diamond crystal while recording the signal. The ATR-FTIR spectra of different stages of membrane functionalization is represented in **Figure S3.** All the characteristic peaks are identified by comparing to the published data[1-6]. The characteristic peaks such as C-F bonds (~1170 cm^{-1}), C-F_2 bonds (~1200 cm^{-1}), and vibration of CH_2 bending (~1400 cm^{-1}) of the blank PVDF membrane for are shown by the blue line in **Figure S3**[1-2]. The appearance of peaks around 1700 cm^{-1} and 1550 cm^{-1} in **Figure S3** (red line) is due to carbonyl stretch and antisymmetric stretching of carboxyl groups (-COOH), respectively, of the polyacrylic acid polymer[3-5]. In addition, the broad peak in **Figure S3** (red line) between 2700 and 3400 cm^{-1} is demonstrating the presence of O-H group from the synthesized polymer[3]. Introduction of EDC/NHS chemistry on PAA-PVDF membrane leads to incorporate amine groups on PAA-PVDF functionalized membrane. The ATR-FTIR spectra of NHS-PAA-PVDF membrane is demonstrated in **Figure S3** (green line). The appearance of a deformation peak centered at 1650 cm^{-1} wavelength could be attributed to amide II bending[6]. The sharp peak around 3300 to 3500 cm^{-1} is due to primary amine stretching. Primary amine produces two N-H stretching while secondary amides yields only one. The absorbance spectra of CysM-PAA-PVDF membrane is depicted in **Figure S3** (pink line). The small amide I band is visible around wavelength 1650 cm^{-1}, however it is smaller compare to the same peak for NHS-PAA-

PVDF membrane, due to incorporation of thiol (-SH) groups in the membrane[6]. In addition, a broad peak in the wavelength range of 2450 cm^{-1} to 3500 cm^{-1} is clearly visible (pink line), which is sharply different than the broad peak of PAA-PVDF membrane (red line). This broad peak is due to overlap of amide II stretching peak and mercaptan (S-H stretching) peak, suggesting covalent attachment of thiol (-SH) groups on PAA-PVDF membrane.

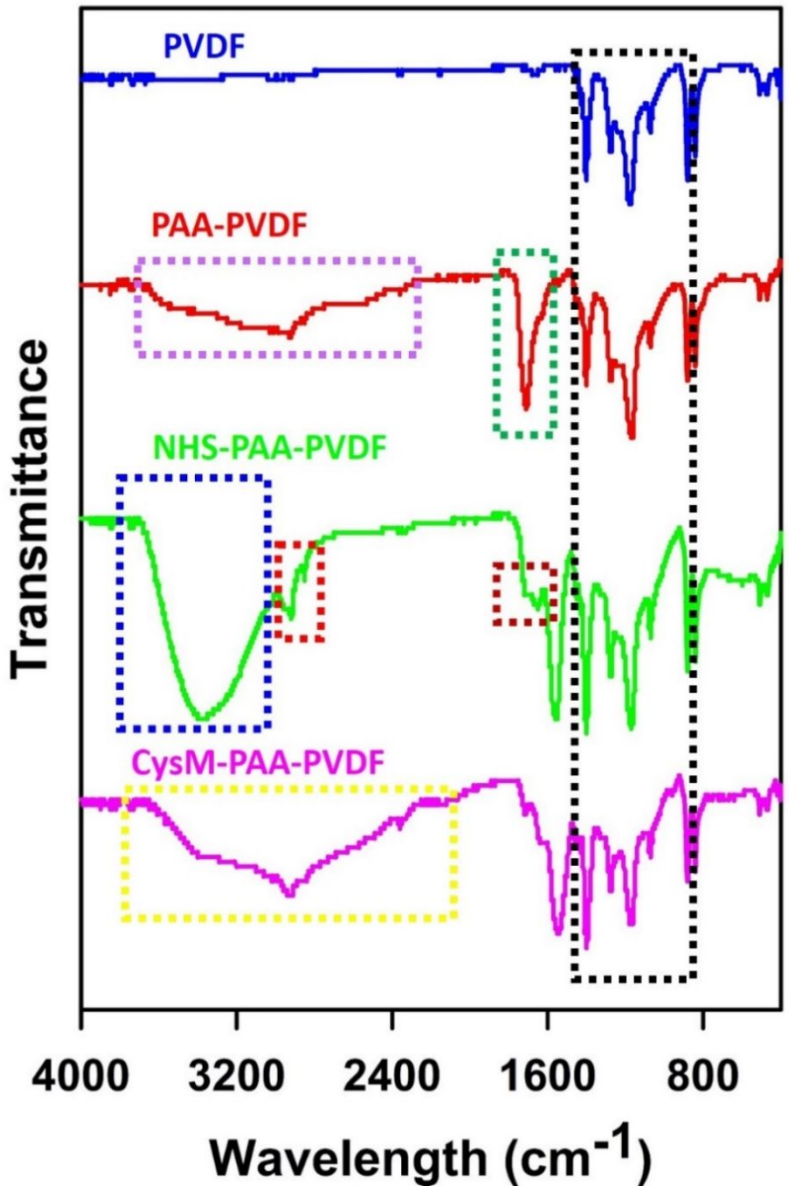

Figure S3: The ATR-FTIR spectra of different stages of functionalization. The blank PVDF membrane is represented by the blue line, The PAA-PVDF membrane (red line) after functionalization of PVDF membrane with acrylic acid to introduce carboxylic groups (-COOH), The NHS-PAA-PVDF membrane (green line) while introducing EDC/NHS chemistry on PAA-PVDF membrane and, finally the CysM-PAA-PVDF membrane (pink line) after incorporation of thiol (-SH) groups in PAA-PVDF membrane.

S5. Reaction Steps of Thiol Membrane

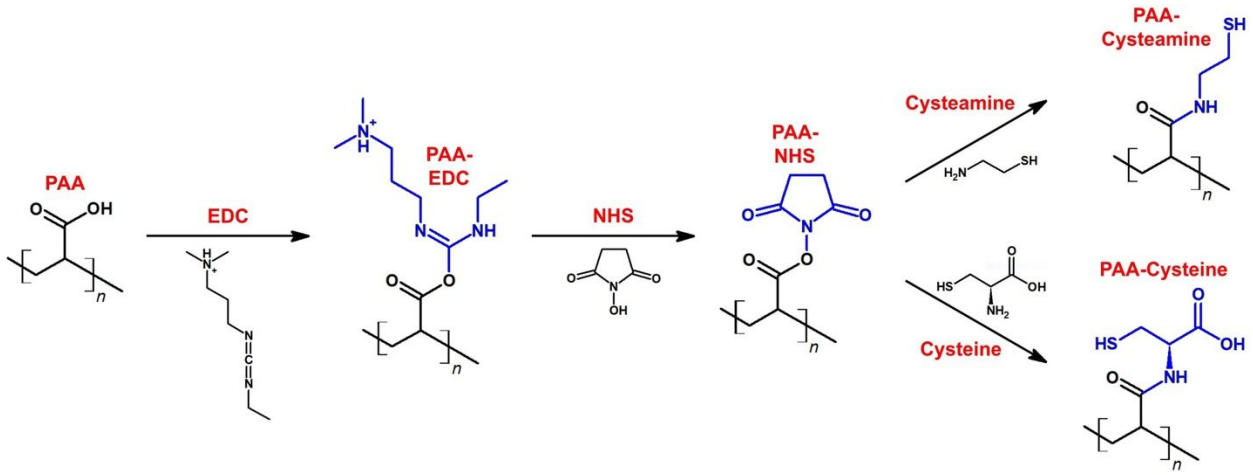

Figure S4: Schematic of reaction steps to functionalize PAA-PVDF membrane with EDC/NHS solution followed by incorporation of thiol (-SH) groups by passing a thiol (-SH) precursor (Cys/CysM) solution.

S6. Adsorption-Desorption Study of Ag^+ and Hg^{2+} Cations on PAA-PVDF Membrane

The PAA-PVDF membrane could adsorb heavy metal ions (Ag^+ and Hg^{2+}) from water as it has carboxylic groups (-COOH) at the end of the polymer chain. The heavy metal ions (Ag^+ and Hg^{2+}) can hydrolyze in wide range of pH and enable to attach with carboxylic groups (-COOH) by replacing H^+ in a suitable pH[7]. However, this attachment is not permanent and by passing a low pH solution through the membrane it could be easily desorbed from the PAA chain of PAA-PVDF membrane. In **Figure S5**, the adsorption-desorption profile is shown for both silver (**Figure S5a**) and mercury (**Figure S5b**). The results on **Figure S5** confirms it is possible to attach and dislodge heavy metals in PAA chain of PAA-PVDF membrane. However, this PAA-PVDF membrane is not suitable for industrial application as if pH changes the heavy metals can easily detached from the PAA chain. It is worth to mention that, not all the Ag^+ and Hg^{2+} cations attached in the PAA chain is not desorbed and a small fraction is permanently remain in the polymeric chain.

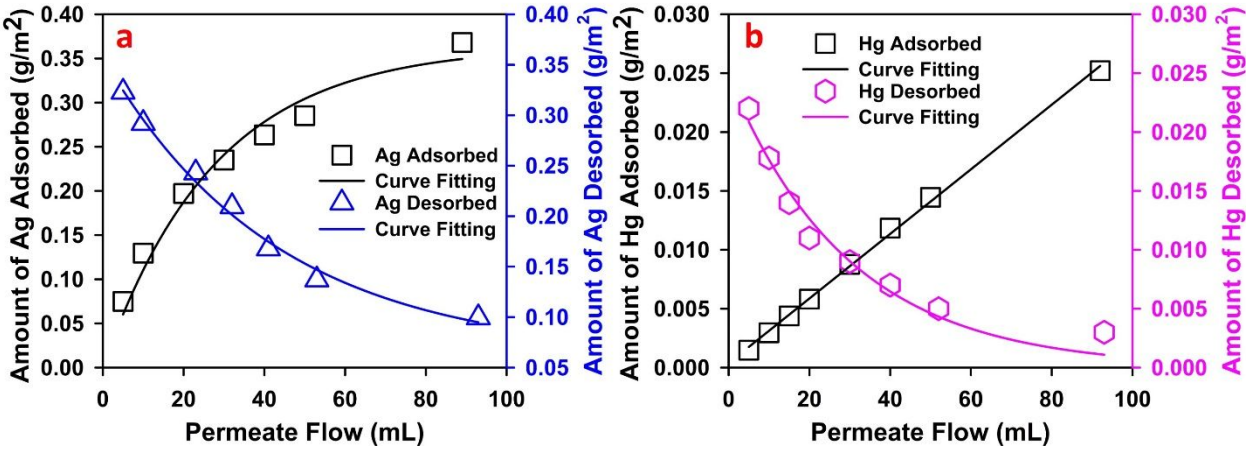

Figure S5: Results of adsorption-desorption study of heavy metal ions (Ag^+ and Hg^{2+}) on PAA-PVDF membrane. **(a)** The adsorption and desorption profile of Ag^+ cations on PAA-PVDF membrane. Membrane mass gain is 3.99%, water flux = 38.38 LMH at 2.04 bar, water pH = 5.2, flux during Ag^+ cations adsorption is 37.92 LMH at 2.04 bar. Ag^+ solution pH = 4.75. The initial concentration of Ag^+ solution is around 20 ppm. The flux during Ag^+ cations desorption is 45.6 LMH at 2.04 bar. Desorption solution pH =3.1, **(b)** The adsorption and desorption profile of Hg^{2+} cations PAA-PVDF membrane. Membrane mass gain is 3.16%, water flux = 18.18 LMH at 2.72 bar, water pH = 5.1, flux during Hg^{2+} cations adsorption is 12.86 LMH at 2.72 bar. Hg^{2+} solution pH = 4.7. The initial concentration of Hg^{2+} solution is around 400 ppb. The flux during Hg^{2+} cations desorption is 21.6 LMH at 2.04 bar. Desorption solution pH =2.9. For both cases the effective membrane surface area is 13.2 cm^2. The cation solution is passed in convective flow mode across the membrane. Silver nitrate ($AgNO_3$) and mercury (II) nitrate hydrate ($Hg(NO_3)_2 \cdot xH_2O$, x= 1-2) salts were used to prepare the cationic solution.

S7. Adsorption Efficiency of Heavy Metals on Thiol Membrane

Once the PAA-PVDF membrane is functionalized with thiol (-SH) groups it can adsorb heavy metals from water. However, not all the thiol groups attached to the membrane will be exposed to adsorb heavy metals from water. The complex geometry of the membrane pores, small channeling to by-pass the attached thiol groups, inherited defects of the membrane pore structure, residence time and fouling with time are the key factors to hinder all the attached thiol groups to capture heavy metals from the solution. In order to study the adsorption efficiency of the heavy metals on thiol functionalized membranes, a CysM-PAA-PVDF membrane is exposed to capture heavy metals from water. Here, Ag^+ cations are used as a model compound and Ag^+ molar attachment to thiol groups is always 1 to 1. The synthetic water is used to avoid interference of adsorption of other cations and fouling. The result of the adsorption efficiency is shown in **Figure S6**.

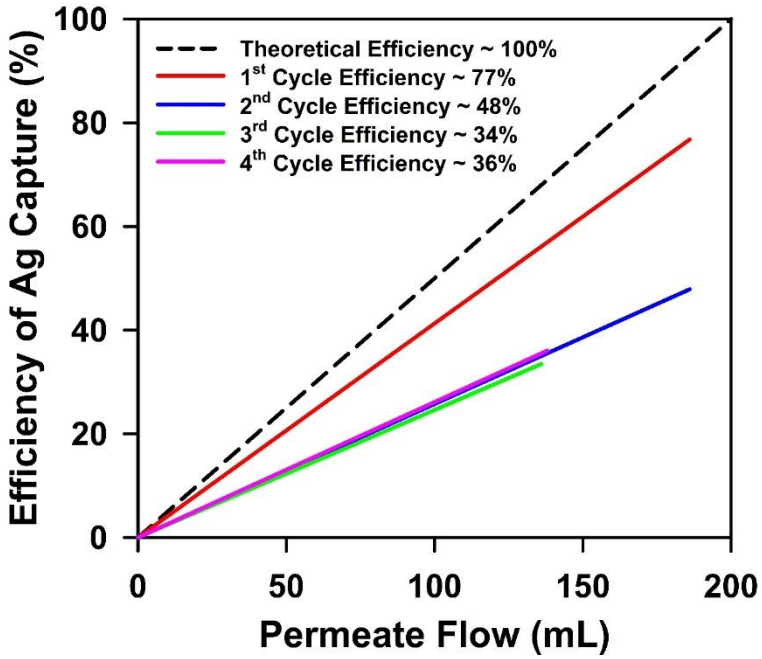

Figure S6: The adsorption efficiency trend to capture Ag^+ cations on CysM-PAA-PVDF membrane. The membrane mass gain was 9.79%. Effective membrane surface area is 13.2 cm^2.The ICP-OES analysis of feed, permeate and retentate samples were used to do mass balance in order to calculate Ag^+ cations capture. Total experiment time was 820 minutes. Silver nitrate ($AgNO_3$) salt is used to prepare the cationic solution. The Ag^+ cation solution pH ~ 5.8 to 6.8. For, first cycle (red line), solution passed = 186 mL, time of operation = 235 minutes, Ag^+ cation concentration in feed = 10 ppm, for second cycle (blue line), solution passed = 186 mL, time of operation = 310 minutes, Ag^+ cation concentration in feed = 30 ppm, for third cycle (green line), solution passed = 136 mL, time of operation = 231 minutes, Ag^+ cation concentration in feed = 30 ppm,, for fourth cycle (pink line), solution passed = 138 mL, time of operation = 241.5 minutes Ag^+ cation concentration in feed = 20 ppm.

The study was conducted for 820 minutes (approximately13.5 hours) by passing around 650 mL Ag^+ cation solution to make the experiment more pragmatic. During the whole experiment the solution permeability is kept constant to a value around 8 LMH/bar. The permeability is kept low to allow more residence time for adsorption of Ag^+ cations. In the first cycle, the calculated adsorption efficiency is around 77% while passing only 190 mL Ag^+ cation solution for 235 minutes (3.9 hours). However, the adsorption efficiency dropped to 48% during second cycle when another 190 mL Ag^+ cation solution passed for 310 minutes (5.16 Hours). For the next two cycles (third and fourth) the adsorption efficiency is almost constant to around 35% on average. The third cycle runs for for 231 minutes (3.85 hours) while passing 136 mL of Ag^+ cation solution and fourth cycle runs for 241.5 minutes (4 hours) passing 138 mL of solution. Though, it is expected the adsorption efficiency should be 100%, however, the factors mentioned earlier of this discussion play a pivotal role to reduce the heavy metal capture efficiency, deviating from the model membrane performance. It is worth to mention here that at initial stage, pore channeling plays a significant role on adsorption efficiency, but in later stage, less accessibility to thiol (-SH) groups on pore vicinity and fouling eventually dominates the adsorption efficiency.

S8. Mercury Adsorption Analysis on CysM-PAA-PVDF Membrane by XPS

The analysis of the XPS spectrum back-up the adsorption of heavy metals (Ag^{+}/Hg^{2+}) on thiol (-SH) functionalized PAA-PVDF membrane. Both survey scan and high-resolution scan were conducted for XPS analysis. The Beta angles (degrees from vertical) of the XPS instrument was as following: monochromator (crystal) 60°, ion gun 58°, flood gun 58° and height adjust microscope 45°, respectively. No tilt was used. The step size was 1 eV and 0.1 eV for survey and high-resolution scan. The pass energy was 200 eV and 50 eV for survey and high-resolution scan. XPS spectra were calibrated (charge correction) to a C1s peak value of 284.8 eV. The XPS survey scan after adsorption of Hg^{2+} on CysM-PAA-PVDF membrane is demonstrated in **Figure S7a** showing the presence of Hg and S peaks over the top surface of the membrane. In addition of Hg and S peaks, the other observed peaks are for the elements C, N, O and F. The characteristic peaks of all the elements (Hg, S, C, N, O and F) are identified by comparing to the available literature data[2, 6, 8-10]. The leftmost peak identified in **Figure S7** around 100 eV is representing the Hg4f. The appearance of this peak is due to the binding of Hg with S of thiol (-SH) group yielding HgS. This is basically doublet peaks at binding energies of 101 and 106 eV which could be attributed to Hg 4f7/2 and Hg 4f5/2, shown separately in **Figure S7b**[6, 8-9]. The next peak around binding energy of 164 eV could be assigned to R-SH binding or to presence of sulfur (S2p) from thiol (-SH) groups[8-9]. Further observed peak around binding energy of 225 eV could be assigned to S2s peak as in this region the expected peak is for Molybdenum (Mo3d). However, in the examined sample there is no scope of presence of Molybdenum. However, it is worth to mention that S2s region strongly overlaps with Mo3d, when sulfur is present as sulfate. The next peak around binding energy of 286 eV is attributed to C1s peak[2, 10]. This is due to the presence of carbon in PVDF membrane, as well as, for the functionalization with AA and cross-linker MBA during incorporation of carboxylic (-COOH) groups in membrane. The N1s peak at binding energy of 400 eV is for N as amide (-NH2) in cross-linker MBA[2, 10]. The O1s peak at binding energy of 532 eV is due to the presence of O in carboxyl groups (-COOH)[2, 10]. The final identified peak at binding energy of 689 eV is for F1s[2]. This peak represents organic F which is present in fluorocarbon groups (-CF2-) of PVDF membrane.

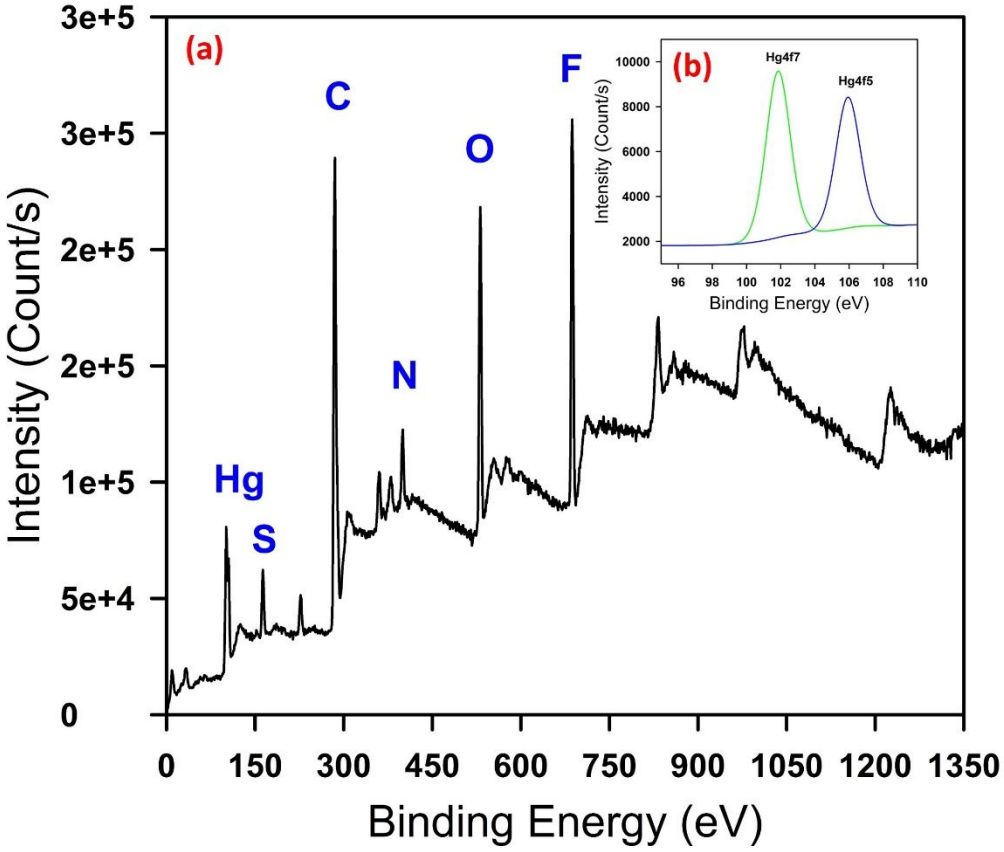

Figure S7: The XPS spectrum of CysM-PAA-PVDF membrane after sorption of Hg^{2+} from industrial effluent water. **(a)** The survey scan is showing the presence of elements Hg, S, C, N, O and F (from left to right), **(b)** The high-resolution scan shows elemental Hg confirmed by doublet peaks (Hg4f7 and Hg4f5).

S9. Results of EDX Analysis of CysM-PAA-PVDF Membrane

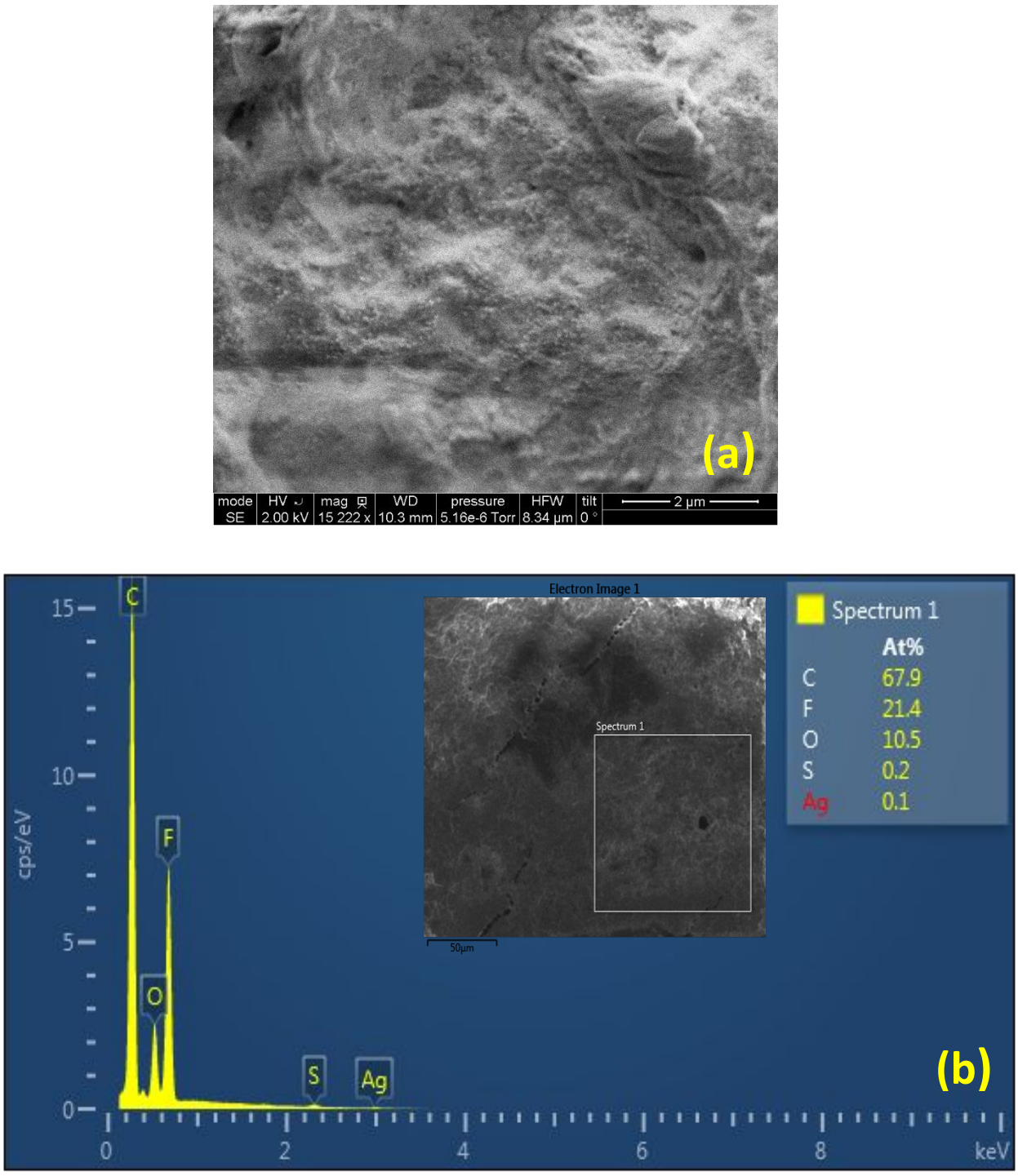

Figure S8: (a) The SEM image of CysM-PAA-PVDF membrane after adsorption of Ag^{+} cations from the solution by convective flow mode, **(b)** the EDX analysis shows the presence of Ag on the surface of CysM-PAA-PVDF membrane along with C, F, O and S. The inset picture is also showing the atomic percentage of C, F, O, S and Ag. The membrane mass gain was 4.49%. The feed concentration was around 90 ppm.

Table S3. Summary of the EDX scanning results for the top surface of CysM-PAA-PVDF membrane after adsorption of Ag^+ cations from the water. The membrane mass gain was 4.49%. The feed concentration of Ag^+ cation solution was around 90 ppm was passed through the membrane in convective flow mode. The solution pH was around 4.8-5.3. The solution was prepared by using $AgNO_3$ salt. The atomic composition of Carbon (C), fluorine (F), oxygen (O), sulfur (S), and silver (Ag) were measured in different locations of the membrane sample during EDX analysis.

Location	C (At%)	F (At%)	O (At%)	S (At%)	Ag (At%)
1	67.87	21.42	10.49	0.15	0.07
2	66.53	22.63	10.56	0.19	0.10
3	66.54	19.89	13.20	0.24	0.13
Average	66.98	21.31	11.42	0.19	0.10
Standard Deviation	0.77	1.37	1.54	0.05	0.03

S10. Materials

All chemicals used during the laboratory-scale membrane fabrication and other studies were of reagent grade and used as received without further purification. Acrylic acid (AA), 98% extra pure and stabilized (ACROS ORGANICS, France); N,N′-Methylenebisacrylamide (MBA), for electrophoresis, 99+% (ACROS ORGANICS, Belgium); potassium persulfate (KPS), min. 99% (EM SCIENCE, Germany). Fluoraldehyde™ o-Phthaldialdehyde Reagent solution, (Product Number (PN): 26025) (Thermo Scientific, Rockford, IL, USA), sodium hydroxide (NaOH) solution (1.0 N), (PN: BDH7222) (VWR Analytical, USA), sodium chloride (NaCl) salt, PN: BDH9286 (VWR Chemicals, Ohio, USA), calcium chloride ($CaCl_2$) salt, ACS Grade, PN: BDH9224, (VWR International, PA, USA), sulfuric acid (H_2SO_4) solution (1.0 N), PN: BDH7232 (VWR Analytical, USA), Nitric acid 68,0 - 70,0%, AR Select® ACS for trace metal analysis, (Macron Fine Chemicals, Center Valley, PA, USA). Ethanol, 99.5%, (PN: EX0276-3) (EMD Millipore Corporation, USA), ammonium persulfate ($(NH_4)_2S_2O_8$), 98+% (Acros Organic, Geel, Belgium), N-(3-Dimethylaminopropyl)-N′-ethylcarbodiimide hydrochloride (EDC), ≥ 98.0% (Sigma-Aldrich, St Louis, MO, USA), and N-hydroxysucinimide (NHS), ($C_4H_5NO_3$), >98.0% (TCI, Tokyo, Japan). Cysteamine hydrochloride (MEA), ≥ 98.0% (Sigma-Aldrich, St Louis, MO, USA), $_L$-Cysteine Hydrochloride; Monohydrate (Cys), ($C_3H_7NO_2.HCl.H_2O$), PN: C-6852 (Sigma-Aldrich, St Louis, MO, USA). Mercury (II) nitrate hydrate ($Hg(NO_3)_2 \cdot xH_2O$, x= 1-2), ACS 98.0% (Alfa Aesar, Ward Hill, MA, USA). Silver Nitrate ($AgNO_3$), Crystal, 99.8-100.5% (PN: JT3429-04), (J. T. Baker, Phillipsburg, NJ, USA). Commercial scale membranes of polyvinylidene fluoride (PVDF, microfiltration 250~400 nm pore size, thickness with backing is around of 174 ± 8 μm (PVDF layer ≈ 70~76 μm) and porosity around 36 - 44%) (PV700 produced in collaboration with Nanostone Water, Inc., USA). Membrane surface area of 13.2 cm^2 were used.

S11. EDC/NHS Functionalization of PAA-PVDF Membrane and Flux Pattern

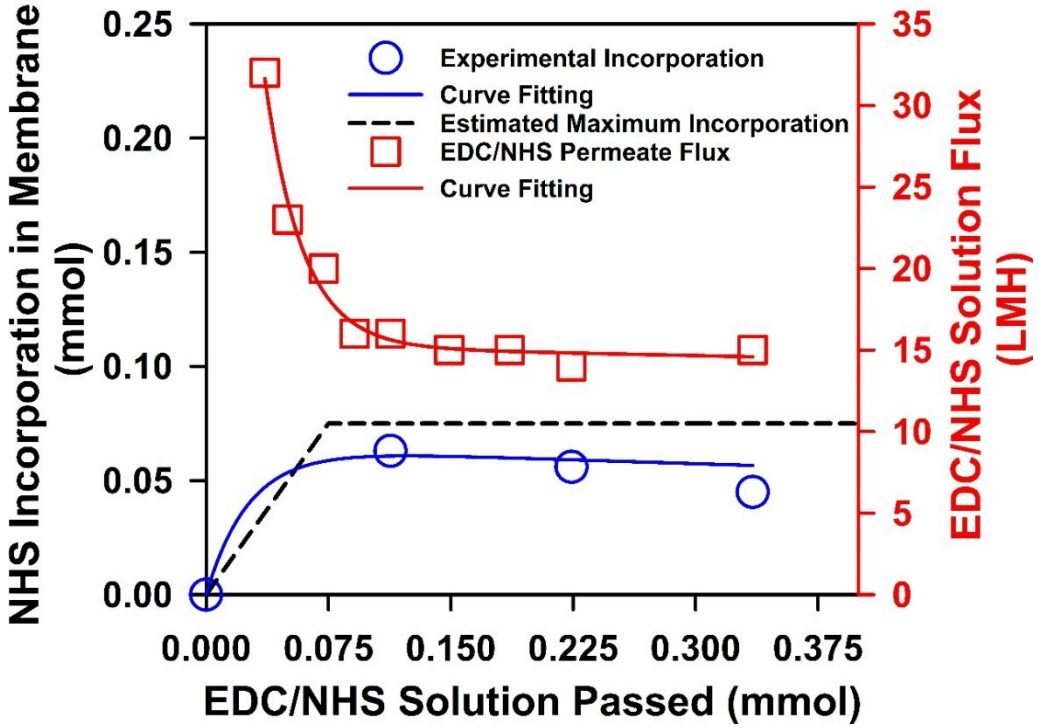

Figure S9: The cumulative amount of NHS added to a PAA-PVDF membrane (surface area 13.2-cm^2) during passing a mixture of 5.0 mM NHS and 5.0 mM EDC solution (pH = 6.3) by convective flow through the membrane. The flux pattern during this EDC/NHS incorporation is shown on the right y-axis. The pressure during experiment was kept around 6.9 ± 0.3 bar. TOC analysis of feed and permeate samples was used to measure the incorporation. The estimated maximum capacity for incorporation was determined based on mass gained by the membrane during PAA functionalization.

S12. Cysteamine (CysM) Incorporation in NHS-PAA-PVDF membrane and Flux Pattern

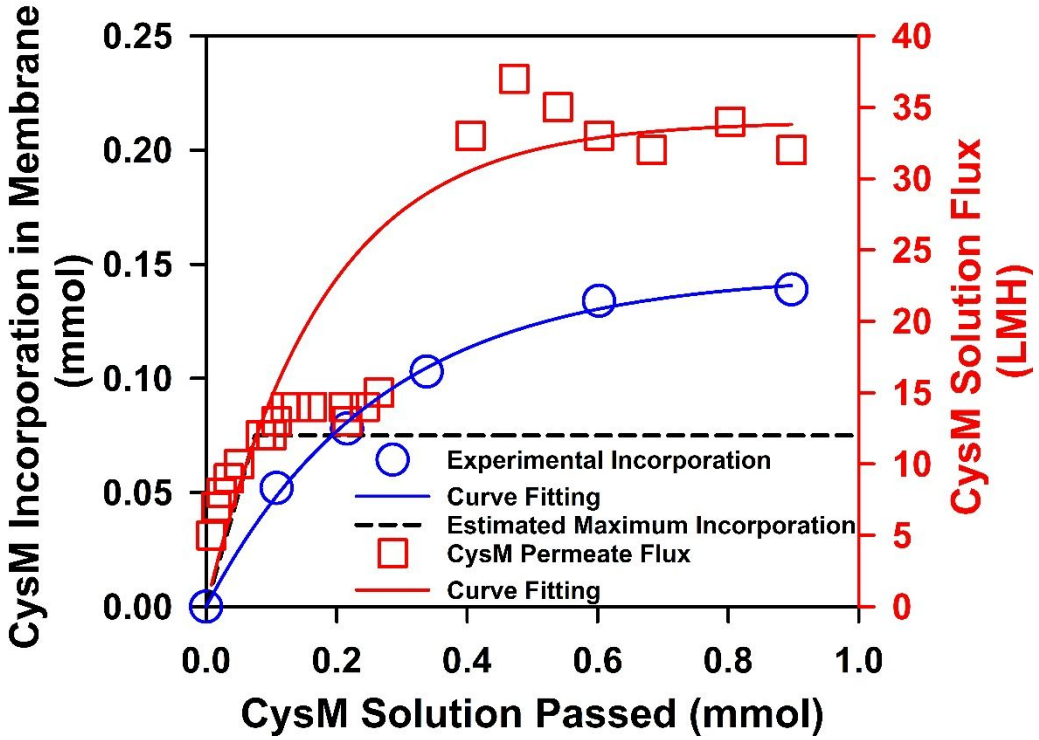

Figure S10: CysM incorporation into an NHS-PAA-PVDF membrane (surface area 13.2-cm^2) during passing a 1.0-g/L, CysM solution (pH = 7.5) by convective flow through the membrane. The flux pattern during this CysM incorporation is shown on the right y-axis. The pressure during experiment was kept around 6.9 ± 0.3 bar. TOC analysis of samples of the feeds and permeates was used to determine the amount of CysM incorporation. The NHS-PAA-PVDF membrane used was obtained by the convective-flow of EDC/NHS solution through the membrane. The estimated maximum capacity for incorporation was determined using the mass gained by the membrane during PAA functionalization.

References:

1. He, F.; Luo, B.; Yuan, S.; Liang, B.; Choong, C.; Pehkonen, S. O., PVDF Film Tethered with RGD-Click-Poly(glycidyl methacrylate) Brushes by Combination of Direct Surface-Initiated ATRP and Click Chemistry for Improved Cytocompatibility. *RSC Adv.* **2014,** *4* (1), 105-117.
2. Islam, M. S.; Hernández, S.; Wan, H.; Ormsbee, L.; Bhattacharyya, D., Role of Membrane Pore Polymerization Conditions for pH Responsive Behavior, Catalytic Metal Nanoparticle Synthesis, and PCB Degradation. *J. Membr. Sci.* **2018,** *555*, 348-361.
3. Kirwan, L. J.; Fawell, P. D.; van Bronswijk, W., In Situ FTIR-ATR Examination of Poly(acrylic acid) Adsorbed onto Hematite at Low pH. *Langmuir* **2003,** *19* (14), 5802-5807.
4. Sarma, R.; Islam, M. S.; Miller, A.-F.; Bhattacharyya, D., Layer-by-Layer-Assembled Laccase Enzyme on Stimuli-Responsive Membranes for Chloro-Organics Degradation. *ACS Appl. Mater. Interfaces* **2017,** *9* (17), 14858-14867.
5. Sarma, R.; Islam, M. S.; Running, M.; Bhattacharyya, D., Multienzyme Immobilized Polymeric Membrane Reactor for the Transformation of a Lignin Model Compound. *Polymers* **2018,** *10* (4), 463.
6. Hernández, S.; Islam, M. S.; Thompson, S.; Kearschner, M.; Hatakeyama, E.; Malekzadeh, N.; Hoelen, T.; Bhattacharyya, D., Thiol-Functionalized Membranes for Mercury Capture from Water. *Ind. Eng. Chem. Res.* **2019**.
7. Baes, C. F.; Mesmer, R. E., *The Hydrolysis of Cations*. John Wiley & Sons: New York, USA, 1976.
8. Huang, L.; Peng, C.; Cheng, Q.; He, M.; Chen, B.; Hu, B., Thiol-Functionalized Magnetic Porous Organic Polymers for Highly Efficient Removal of Mercury. *Ind. Eng. Chem. Res.* **2017,** *56* (46), 13696-13703.
9. Zhang, X.; Wu, T.; Zhang, Y.; Ng, D. H. L.; Zhao, H.; Wang, G., Adsorption of Hg^{2+} by Thiol Functionalized Hollow Mesoporous Silica Microspheres with Magnetic Cores. *RSC Adv.* **2015,** *5* (63), 51446-51453.
10. Wang, W.; Lu, Y.-C.; Huang, H.; Wang, A.-J.; Chen, J.-R.; Feng, J.-J., Solvent-free Synthesis of Sulfur- and Nitrogen-co-doped Fluorescent Carbon Nanoparticles from Glutathione for Highly Selective and Sensitive Detection of Mercury(II) Ions. *Sens. Actuators, B* **2014,** *202*, 741-747.